

Bridging the gap between atmospheric concentrations and local ecosystem measurements

T. Lauvaux^{1,3,10*}, B. Gioli², C. Sarrat³, P. J. Rayner¹, P. Ciais¹, F.

Chevallier¹, J. Noilhan³, F. Miglietta², Y. Brunet⁷, E. Ceschia⁶, H. Dolman⁴,

J. A. Elbers⁸, C. Gerbig⁵, R. Hutjes⁸, N. Jarosz⁶, D. Legain³, M. Uliasz⁹

1

Laboratoire des Sciences du Climat et de l'Environnement, Gif-sur-Yvette, France

2

CNR, Institute of Biometeorology, Florence, Italy

3

CNRM, Météo France, Toulouse, France

4

Vrije Universiteit, Amsterdam, Netherlands

5

Max Planck Institute for Biogeochemistry, Jena, Germany

6

CESBIO, Toulouse/Auch, France

7

INRA, EPHYSE, Bordeaux, France

8

Alterra, Wageningen, Netherlands

9

Colorado State University, Fort Collins, Colorado

10

Now at Pennsylvania State University, Department of Meteorology, State College, Pennsylvania

T. Lauvaux, Pennsylvania State University, Department of Meteorology, 418B Walker Building,
State College, PA 16802 (lauvaux@meteo.psu.edu)

This paper presents the first direct comparison of regional CO₂ fluxes estimated by inversion of atmospheric concentration data with fluxes measured by towers and aircraft. All measurements were made in a 300×300km domain in southwest France in 2005. Concentrations were measured on two short towers while fluxes were measured on 5 towers and 27 aircraft transects. The inversion produces a better fit than the prior estimate to the measured fluxes, capturing both the temporal evolution and behaviour of different ecosystems. Additionally, the final estimate is most improved where the theoretical error reduction is highest. Results suggest that atmospheric inversion is a reliable tool for estimating regional CO₂ fluxes provided the components are verified.

1. Introduction

Atmospheric inversions of CO₂ surface sources have played a key role in quantifying large-scale sources and sinks of CO₂ [e.g. Tans *et al.*, 1990; Gurney *et al.*, 2002; Baker *et al.*, 2007]. There are no direct measurements of CO₂ flux at these scales so the information cannot be verified. This paper attempts such a verification. We immediately face a problem of scale since we need sufficiently dense flux measurements to obtain spatial estimates comparable with the atmospheric inversions. During the CarboEurope Regional Experiment Strategy (CERES) in Southern France [Dolman *et al.*, 2006], CO₂ fluxes were measured locally by the eddy covariance technique at five sites chosen to represent regional ecosystem types and also spatially by aircraft flying just above the surface. In addition, two towers measured continuously CO₂ concentrations. Eddy-flux measurements are completely independent of the inversion and are kept as validation data for the inverse fluxes. Inverse fluxes are calculated at 8km resolution over 6-day periods using hourly CO₂ measurements and high-resolution transport modelling. The temporal resolution is a compromise due to the lack of data (only two towers) but still uses the information from hourly concentrations. Sarrat *et al.* [2007b] and Lauvaux *et al.* [2008b] demonstrated the capability of the model to assimilate such observations.

The outline of the paper is as follows: In section 2 we briefly describe the tools and datasets underlying the study. Section 3 describes the major results while Section 4 considers some implications and summarises the results.

2. Inverse system and independent flux measurements

The study period consists of 18 days in 2005 divided into 3 intensive observing periods, IOP-1 (May 24–29), IOP-2 (May 30–June 4) and IOP-3 (June 5–10). We estimate mean daytime fluxes for each IOP at $8 \times 8 \text{ km}$ resolution (between 8am and 8pm). Hourly concentrations were measured on two towers throughout the period, at Biscarosse, located on the Atlantic coast at 50 m height on a 70 m hill, and Marmande, inland, at a height of 20 m in an agricultural region (fig. 1). Influence functions of these two towers, describing the relation between surface fluxes and concentrations, were calculated using the non hydrostatic atmospheric model Meso-NH [Lafore *et al.*, 1998] coupled to the Lagrangian model LPDM [Uliasz, 1994]. Meso-NH was run at 8 km resolution with 65 levels describing the atmospheric column up to 13 km . The first vertical level represents the lowest 20 m of the atmospheric column. The Lagrangian model LPDM is coupled offline to MesoNH, as described in Lauvaux *et al.* [2008b]. The typical surface flux area influencing the tower's concentration measurement extends 300 km from the Atlantic Ocean to the Mediterranean coast (fig. 1, upper right corner, in red). The first guess fluxes were computed each hour with the ISBA-A-gs land surface model [Calvet *et al.*, 1998] at 8 km resolution, forced by the SAFRAN meteorological analyses [Durand *et al.*, 1993]. Concentration boundary conditions from the inversion come from a run of the LMDZ global model [Sadourny and Laval, 1984]. Boundary conditions are included in the inversion but have little impact [Lauvaux *et al.*, 2008b].

We estimated the magnitudes and structures of the observation error covariance matrix by comparing direct simulations with atmospheric measurements [Lauvaux *et al.*, 2008b] and their spatial structure from ensemble analyses [Lauvaux *et al.*, 2008a]. For the prior

flux error covariances, we estimated the correlations of the differences between the ISBA simulation and measurements at 11 flux towers, from the method proposed by [Chevallier *et al.*, 2006]. Only agricultural towers showed evidence of correlated flux errors which are introduced in the inversion setup as a correlation length of 50km for summer crops and winter crops.

During the study period, 27 airborne transects were made to measure CO₂ surface fluxes over the same paths (fig. 1). Fluxes were measured with the eddy covariance technique by a Sky Arrow 650 ERA - Environmental Research Aircraft as described by Gioli *et al.* [2004]. Figure 1 illustrates the two airborne flux transects over the pine-forest ecosystem of *Les Landes* and the agricultural area of *Marmande*. The incoming photosynthetically active radiation (PAR) was used to extend the instantaneous aircraft measurements to 6-day daytime flux averages using the method from Gilmanov *et al.* [2007]. All flights were made at low altitude, ranging from 80 to 100m above the surface. During IOP-1 and IOP-3, the average measurement frequency is about 50 samples for each hour and 20 for IOP-2. Spatial averaging produces aggregated fluxes at about 4km scale and it is these that we compare with our inversions. Even though the inversion scale is larger (8km), they both remain much larger than the average agricultural plot scale (about 0.3km) which avoids representation error. For these larger scales, the corresponding ecosystem is the dominant type that covers at least 30% of the pixel. We selected five instrumented flux towers corresponding to the ecosystem types of the aircraft paths, Auradé and Lamasquère (cereals), Marmande and Saint Sardos (maize), at 2 to 6m height, and Le Bray (pine

forest) at 40m height to characterize the representative ecosystems of the flights over the region.

3. Results

We compare the errors of prior and posterior NEE from the airborne observations. The temporal resolution is limited to 6 days by the scarcity of concentration observations. Figure 2 shows the 6-day mean corrected fluxes during the day for the forest ecosystems (deciduous and coniferous types), and agricultural ecosystems composed by winter crops (C₃, mainly cereals) and summer crops (C₄, mainly maize), with their associated standard deviations. The three IOP show significant trends in the averaged daytime NEE from both aircraft and ecosystem site flux data, corresponding to the rapid growth of summer crops starting in the IOP-3 (5 to 10 June). The trend in airborne NEE of increasing CO₂ uptake resembles the C₄ crop ecosystem flux measurements (from $-3 \mu\text{mol}\cdot\text{m}^{-2}\cdot\text{s}^{-1}$ for IOP-1 to $-8 \mu\text{mol}\cdot\text{m}^{-2}\cdot\text{s}^{-1}$ for IOP-2). The C₃ crop flux site NEE shows a decrease of the CO₂ uptake (from -11 to $-8 \mu\text{mol}\cdot\text{m}^{-2}\cdot\text{s}^{-1}$).

Posterior NEE is closer to the airborne observations than is the prior for 9 out of 14 combinations of ecosystem and all the IOP shown in Fig. 2. Even though prior NEE is better for the forest than for the crops (only 2 to $4 \mu\text{mol}\cdot\text{m}^{-2}\cdot\text{s}^{-1}$ error, *i.e.* 50% of the absolute NEE), the posterior NEE still lies closer to the ecosystem observations. Posterior errors are 20% to 50% less than prior errors. The improvement occurs despite only having two concentration measurement series.

At 8km grid resolution, 14 inversion grid points lie on the two repeated aircraft transects (fig.1). Fig. 3 shows the corrected fraction ρ of the initial misfit ($\rho = (\varepsilon_{\text{corrected}} -$

$\varepsilon_{firstguess})/\varepsilon_{firstguess}$ with $\varepsilon = |NEE_{model} - NEE_{observed}|$ (the model-data mismatch) at these locations. Negative values indicate an improvement. This metric penalizes cases with good priors such as the *Les Landes* forest (Western transect). The agricultural area (Eastern transect) shows better agreement for all locations (from 10 to 60% of reduction of the initial misfit). Both first guess and corrected flux estimates lie close to the flux measurements relative to the posterior uncertainty.

We finally combine the spatial and temporal comparisons into an overall statistical measure of inversion performance. Fig 4 shows this statistical comparison for all the verification ecosystem NEE measurements and the inversion during daytime. Along the x-axis (from left to right), we show the prior misfit averaged over all the aircraft locations (with its standard deviation) and the same estimate after the inversion, and finally the two types of observations (aircraft and towers). The inversion decreases first guess misfit from 4 to 2 $\mu\text{mol}\cdot\text{m}^{-2}\cdot\text{s}^{-1}$ (25% of the mean NEE) and reduces the NEE error by 15% over the area visible to the atmosphere (fig. 1). The error bars represent the mean square error of the prior/posterior divided by their respective uncertainty variances. This ratio tests the consistency of the inversion since it requires that, where the posterior error is smallest (i.e. the atmosphere provides most information) the match to independent flux measurements is most improved. The improvement in corrected fluxes is hence larger than the decrease of flux uncertainty suggesting that transport model error was slightly overestimated by the concentration data comparison.

4. Discussion and conclusions

The results suggest that when compared to direct flux measurements at comparable scales, this atmospheric inversion significantly improves the prior estimates; even where the prior is fairly good. Improvement occurs for both spatial structure and time evolution. This is true despite only having two concentration timeseries and despite the heterogeneity of the landscape.

One reason for the apparent success may be that the major components of the inversion system had been previously tested and the relevant uncertainties assigned accordingly. Prior uncertainties were assigned by comparison with observations. The uncertainties on data were set by considering the mismatch between simulations and observations calculated by Sarrat *et al.* [2007a]; Lauvaux *et al.* [2008b] using the prior fluxes. This is a conservative choice since some of this mismatch comes from errors in the prior flux. We also accounted for some of the uncertainty in transport [Lauvaux *et al.*, 2008a]. Finally Lauvaux *et al.* [2008b] has also shown that much of the domain is observable from the two measurement sites. Our results suggest that, if these conditions: reasonable prior, good transport and reasonable signal are met the inversion is likely to produce meaningful results.

Finally, this study supports the use of aircraft flux measurements. Such measurements seem to be less constrained by representation problems than pointwise flux tower measurements. Although they cannot be used as a routine tool for monitoring regional fluxes, a combination of flux towers validating aircraft fluxes which in turn validate atmospheric inversions seems to provide the link between small and large scales required for quantifying and understanding regional carbon balances.

Acknowledgments. We wish to thank all participants in the CERES campaign for making their data freely available (<http://carboregional.mediasfrance.org/campagne/index>). This work was funded by the European Commission, Sixth Framework Programme, Contract No. GOCE-CT-2003-505572.

References

- D. F. Baker, R. M. Law, K. R. Gurney, P. Rayner, P. Peylin, A. S. Denning, P. Bousquet, L. Bruhwiler, Y.-H. Chen, P. Ciais, I. Y. Fung, M. Heimann, J. John, T. Maki, S. Maksyutov, K. Masarie, M. Prather, B. Pak, S. Taguchi, , and Z. Zhu. Transcom 3 inversion intercomparison: Impact of transport model errors on the interannual variability of regional CO₂ fluxes, 1988-2003. *Global Biogeochem. Cycles*, 20:439, 2007.
- J. C. Calvet, J. Noilhan, J. L. Roujean, P. Bessemoulin, M. Cabelguenne, A. Olioso, and J. P. Wigneron. An interactive vegetation SVAT model tested against data from six contrasting sites. *Agri. and Forest Met.*, 92:73–95, 1998.
- F. Chevallier, N. Viovy, M. Reichstein, and P. Ciais. On the assignment of prior errors in bayesian inversions of CO₂ surface fluxes. *Geophys. Res. Let.*, 33:L13802, 2006. doi:10.1029/2006GL026496.
- A. J. Dolman, J. Noilhan, P. Durand, C. Sarrat, A. Brut, B. Piguet, A. Butet, N. Jarosz, Y. Brunet, D. Loustau, E. Lamaud, L. Tolk, R. Ronda F. Miglietta, B. Gioli, V. Magliulo, M. Esposito, C. Gerbig, S. Körner, P. Galdemard, M. Ramonet, P. Ciais, B. Neininger, R. W. A. Hutjes, J. A. Elbers R. Macatangay, O. Schrems, G. Pérez-Landa, M. J. Sanz, Y. Scholz, G. Facon, E. Ceschia, and P. Beziat. CERES, the carboeurope regional experiment strategy in Les Landes, South West France, may-june

2005. *Bull. Am. Meteorol. Soc.*, pages doi:10.1175/BAMS-87-10-1367, 2006.

Y. Durand, E. Brun, L. Mérindol, G. Guyomarc'h, B. Lesaffre, and E. Martin. A meteorological estimation of relevant parameters for snow models. *Ann. Glacio.*, 18:65–71, 1993.

T.G. Gilmanov, J.E. Soussana, L. Aires, V. Allard, C. Ammann, M. Balzarolo, Z. Barcza, C. Bernhofer, C.L. Campbell, A. Cernusca, A. Cescatti, J. Clifton-Brown, B.O.M. Dirks, S. Dore, W. Eugster, J. Fuhrer, C. Gimeno, T. Gruenwald, L. Haszpra, A. Hensen, A. Ibrom, A.F.G. Jacobs, M.B. Jones, G. Lanigan, T. Laurila, A. Lohila, G. Manca, B. Marcolla, Z. Nagy, K. Pilegaard, K. Pinter, C. Pio, A. Raschi, N. Rogiers, M.J. Sanz, P. Stefani, M. Sutton, Z. Tuba, R. Valentini, M.L. Williams, and G. Wohlfahrt. Partitioning european grassland net ecosystem CO₂ exchange into gross primary productivity and ecosystem respiration using light response function analysis. *Agr. Ecosyst. Environ.*, 121:93–120, 2007.

B Gioli, F. Miglietta, B. De Martino, R.W.A. Hutjes, H.A.J. Dolman, A. Lindroth, M. Schumacher, M. J. Sanz, G. Manca, A. Peressotti, and E. J. Dumas. Comparison between tower and aircraft-based eddy covariance fluxes in five european regions. *Agricultural and Forest Meteorology*, 127(1-2):1–16, 2004.

K. R. Gurney, R. M. Law, A. S. Denning, P. J. Rayner, D. Baker, P. Bousquet, L. Bruhwiler, Y.-H. Chen, P. Ciais, S. Fan, I. Y. Fung, M. Gloor, M. Heimann, K. Higuchi, J. John, T. Maki, S. Maksyutov, K. Masarie, P. Peylin, M. Prather, B. C. Pak, J. Randerson, J. Sarmiento, S. Taguchi, T. Takahashi, and C.-W. Yuen. Towards robust regional estimates of CO₂ sources and sinks using atmospheric transport models. *Nature*,

415:626–630, 2002.

J. Lafore, J. Stein, P. Bougeault, V. Ducrocq, J. Duron, C. Fischer, P. Hereil, P. Mascart, V. Masson, J. P. Pinty, J. Redelsperger, E. Richard, and J. V. de Arellano. The Meso-NH atmospheric simulation system. Part I: adiabatic formulation and control simulations. *Ann. Geophys.*, 16:90–109, 1998.

T. Lauvaux, O. Pannekoucke, C. Sarrat, F. Chevallier, P. Ciais, J. Noilhan, and P. J. Rayner. Structure of the transport uncertainty in mesoscale inversions of CO₂ sources and sinks using ensemble model simulations. *Biogeosciences Discuss.*, 5(6):4813–4846, 2008.

T. Lauvaux, M. Uliasz, C. Sarrat, F. Chevallier, P. Bousquet, C. Lac, K. J. Davis, P. Ciais, A. S. Denning, and P. Rayner. Mesoscale inversion: First results from the CERES campaign with synthetic data. *Atmos. Chem. Phys.*, 8:3459–3471, 2008.

R. Sadourny and K. Laval. *January and July performance of the LMD general circulation model in New perspectives in Climate Modeling*. Elsevier, Amsterdam, 1984.

C. Sarrat, J. Noilhan, A. J. Dolman, C. Gerbig, R. Ahmadov, L. F. Tolk, A. G. C. A. Meesters, R. W. A. Hutjes, H. W. Ter Maat, G. Pérez-Landa, and S. Donier. Atmospheric CO₂ modeling at the regional scale: an intercomparison of 5 meso-scale atmospheric models. *Biogeosciences*, 4(6):1115–1126, 2007.

C. Sarrat, J. Noilhan, P. Lacarrère, S. Donier, H. Dolman, C. Gerbig, P. Ciais, and A. Butet. Atmospheric CO₂ modeling at the regional scale: Application to the Carboeurope Regional Experiment. *Geophys. Res. Lett.*, 112:D12105, 2007.

P. P. Tans, I. Y. Fung, and T. Takahashi. Observational constraints on the global atmospheric CO₂ budget. *Science*, 247:1431–1438, 1990.

M. Uliasz. Lagrangian particle modeling in mesoscale applications. *Environmental Modelling II*, ed. P. Zanetti, Computational Mechanics Publications:71–102, 1994.

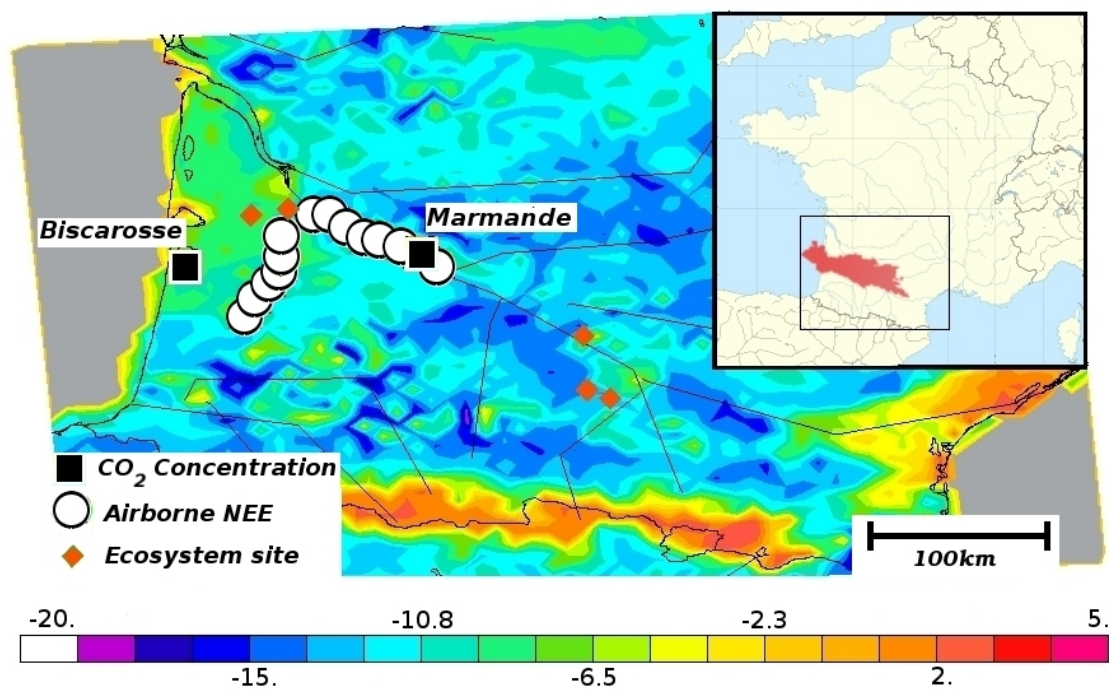


Figure 1. Averaged daytime NEE (in $\mu\text{mol.m}^{-2}.\text{s}^{-1}$) from ISBA vegetation scheme (first guess) for IOP-1) with the two concentration towers (black squares), the CO₂ flux towers (red diamonds), and the aircraft surface footprint (white circles). The influence function of the two concentration towers for IOP-1 is indicated in red on the map (upper right corner)

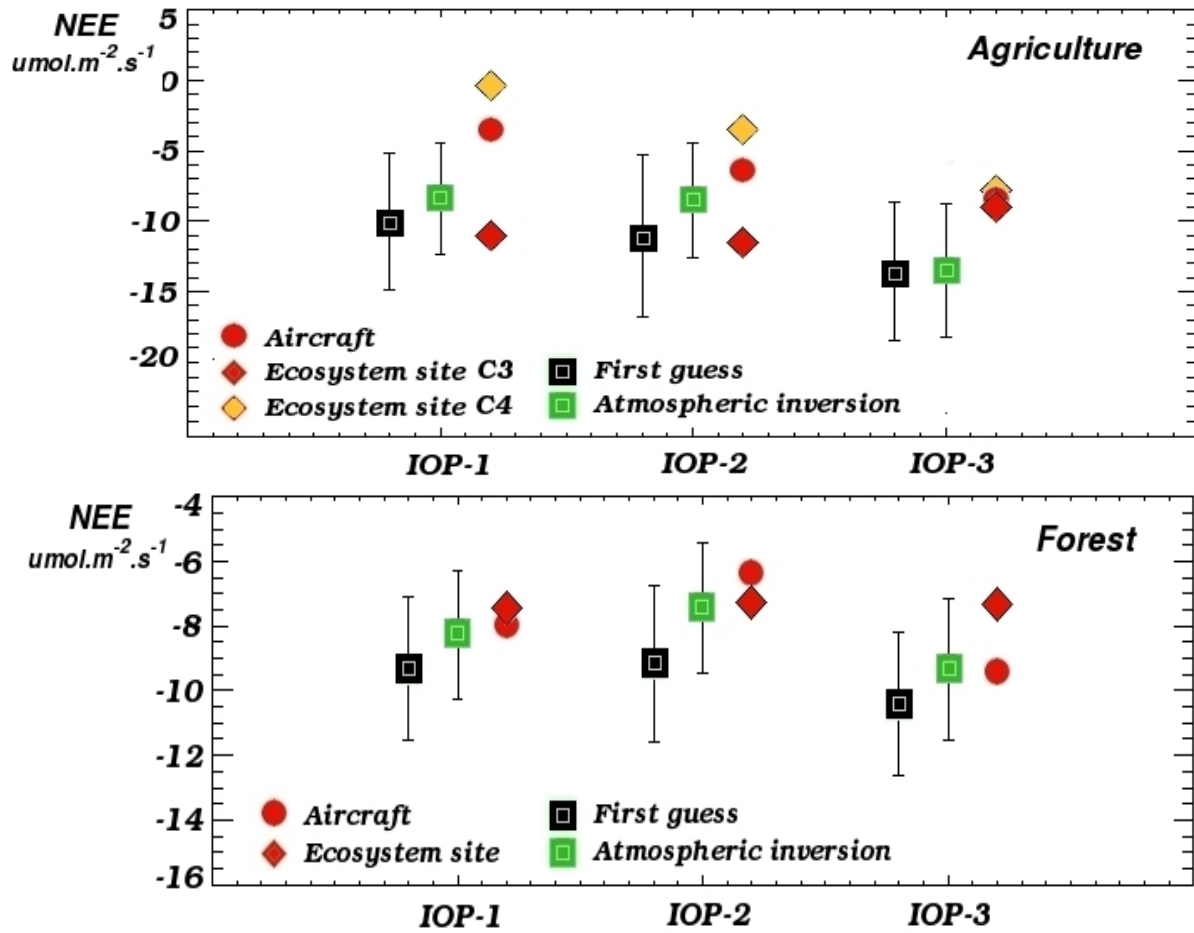


Figure 2. Averaged daytime NEE (in $\mu\text{mol.m}^{-2}.\text{s}^{-1}$) from the land surface model (first guess) and the corrected fluxes compared to the daytime NEE observed from the aircraft and the 5 flux towers for agricultural area fluxes (left) with summer and winter crops (aggregated in the aircraft flux), and forest ecosystem fluxes (right) including deciduous and coniferous forest types in the model (first guess and corrected fluxes)

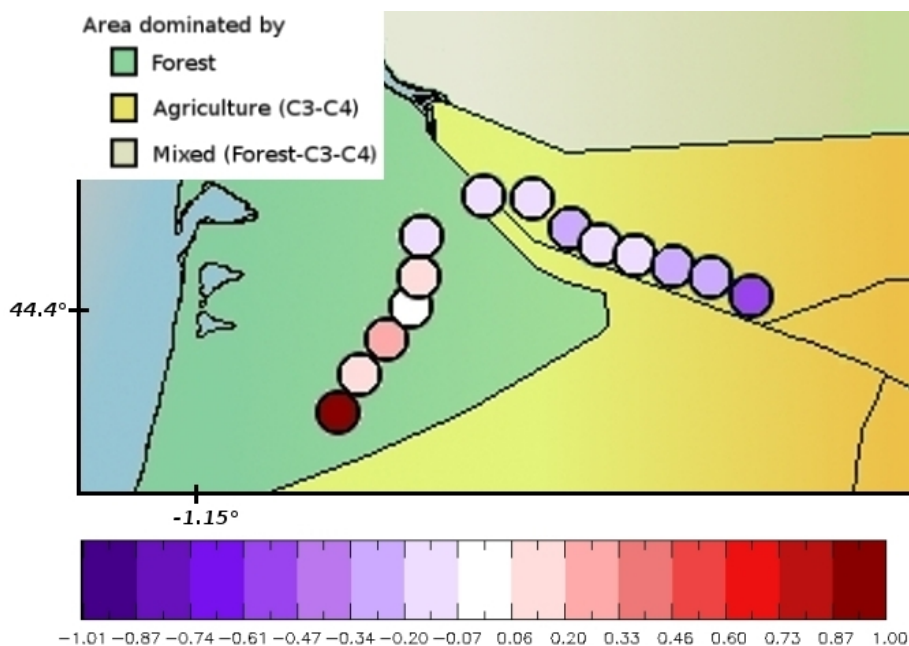


Figure 3. Normalized fractions ρ of the inverse daytime NEE at the aircraft locations, negative if improved (reduction of the initial misfit) and positive when degraded, *i.e.* ratios of the difference between the corrected fluxes and the aircraft ($\varepsilon_{corrected}$) minus the first guess and the aircraft ($\varepsilon_{firstguess}$) normalized by the prior misfit ($(\varepsilon_{corrected} - \varepsilon_{firstguess})/\varepsilon_{firstguess}$). The area dominated by forest ecosystem types is indicated in green, by agriculture in orange, and mixed forest with crops in grey.

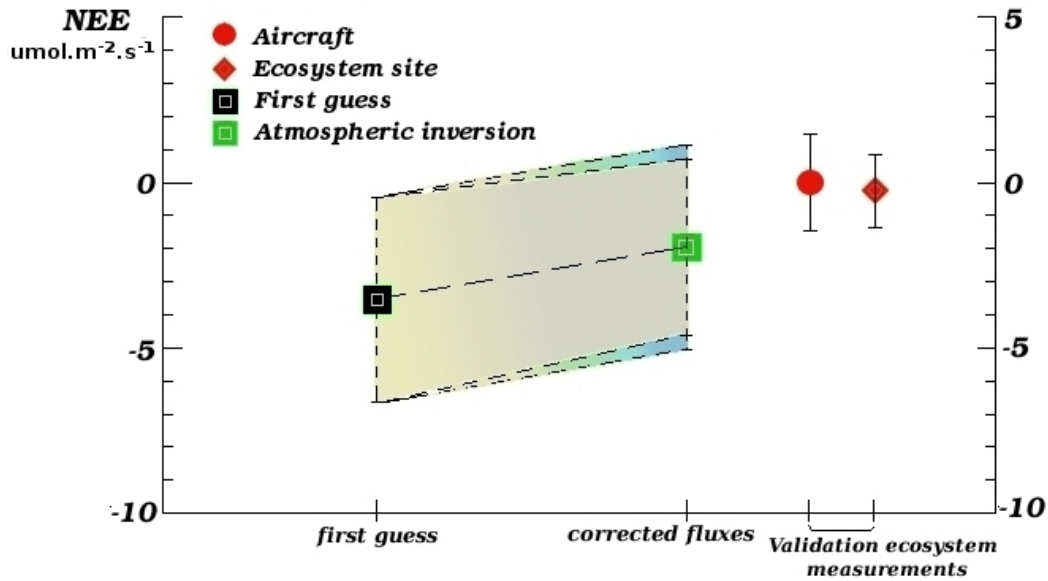


Figure 4. Comparison of the model misfit for the prior (first guess from the vegetation model ISBA-A-gs) and the posterior (corrected fluxes from the inversion) of daytime NEE (in $\mu\text{mol.m}^{-2}.\text{s}^{-1}$) to the aircraft and tower flux data (aircraft NEE being the reference, equal to 0). At each aircraft flux location, the normalized distance was summed, indicated on the figure as error bars, $\Sigma = \frac{(NEE_{\text{model}} - NEE_{\text{aircraft}})^2}{(\sigma_{NEE_{\text{model}}})^2}$, the standard deviation of the χ^2 distribution law. The fit between error reduction and improvement of the flux estimate is shown by the decrease of the normalized distance of the posterior NEE. Estimates have no x-axis correspondence.